PNAS RESEARCH ARTICLE | BIOPHYSICS AND COMPUTATIONAL BIOLOGY

Structural basis of SecA-mediated protein translocation

Linlin Dong[a], Song Yang[b], Jingxia Chen[a], Xiaofei Wu[a], Dongjie Sun[a,1], Chen Song[b,2], and Long Li[a,2]

Edited by Wei Yang, NIH, Bethesda, MD; received May 10, 2022; accepted November 30, 2022

Secretory proteins are cotranslationally or posttranslationally translocated across lipid membranes via a protein-conducting channel named SecY in prokaryotes and Sec61 in eukaryotes. The vast majority of secretory proteins in bacteria are driven through the channel posttranslationally by SecA, a highly conserved ATPase. How a polypeptide chain is moved by SecA through the SecY channel is poorly understood. Here, we report electron cryomicroscopy structures of the active SecA–SecY translocon with a polypeptide substrate. The substrate is captured in different translocation states when clamped by SecA with different nucleotides. Upon binding of an ATP analog, SecA undergoes global conformational changes to push the polypeptide substrate toward the channel in a way similar to how the RecA-like helicases translocate their nucleic acid substrates. The movements of the polypeptide substrates in the SecA–SecY translocon share a similar structural basis to those in the ribosome–SecY complex during cotranslational translocation.

SecA | SecY channel | protein translocation

Significance

The vast majority of secretory proteins in bacteria are translocated across the cell membranes through the SecY channel by a highly conserved ATPase, SecA. We report the structures of the active SecA–SecY with a moving protein substrate in both ADP (adenosine diphosphate) and ATP (adenosine triphosphate) states. The structures reveal that SecA moves protein substrates using an unexpected mechanism that is strikingly similar to how helicases move DNA/RNA substrates. Common structural features are shared by the active SecA–SecY complex and other protein translocation systems targeted by antibiotics, suggesting that SecA could be a highly potent target for antibiotic development against both gram-positive and gram-negative bacteria.

Secretory proteins are translocated across lipid membranes via the ubiquitous Sec translocation system in both prokaryotes and eukaryotes (1). The protein-conducting channel is named the SecY complex in prokaryotes (2, 3) and the Sec61 complex in eukaryotes (4, 5). The channel opens a cross-membrane path for polypeptide substrates during translocation (6). Ribosomes bind to the SecY/Sec61 channel and deliver nascent polypeptide chains to the channel for cotranslational translocation (7). The peptide exit tunnel of the ribosome and the central path of SecY/Sec61 are well aligned in the ribosome–channel complex (8–10). Peptide elongation during translation provides the driving force for the nascent chain to exit from the ribosome and move through the channel. On the other hand, most bacterial secretory proteins follow the posttranslational translocation pathway, in which proteins are completely synthesized before being moved through the channel by a highly conserved ATPase, SecA (11).

SecA belongs to a family of dimeric RecA-like motor ATPases, the members of which are mostly DNA/RNA helicases (12). Similar to the helicases in the family, SecA has two RecA-like nucleotide-binding domains (NBD1 and NBD2) and one nucleotide-binding site that is located between the two NBDs (13) (*SI Appendix*, Fig. S1*A*). A peptide cross-linking domain (PPXD) in SecA has been shown to interact with polypeptide substrates and the SecY channel (14). A helical scaffold domain (HSD) contains a long α-helix spanning the protein and a two-helix finger (THF) motif that penetrates into the cytoplasmic cavity of SecY in the SecA–SecY complex (15, 16) (*SI Appendix*, Fig. S1*B*). A helical wing domain (HWD) is connected to the HSD and located at the opposite side of the protein from the NBDs. During protein translocation, the polypeptide substrates enter SecA through a clamp that is formed between a PPXD loop (residues 326 to 331, PP loop) and two connecting β-strands that link NBD1 and the PPXD (residues 219 to 224 and 351 to 356, TCβ) (17) (*SI Appendix*, Fig. S1*A*).

The helicases in the same family as SecA have been studied extensively for their translocation mechanism (18). These RecA-like ATPases, such as pcrA (19), UvrD (20), and RecD2 (21), translocate along single-strand DNA/RNA using the "inchworm" mechanism (22). The closing and opening of the two NBDs upon ATP binding and hydrolysis are coupled with the alternating binding of the two NBDs to the DNA/RNA strand. Energy from ATP hydrolysis is converted to the translocation steps of the NBDs along the nucleic acid substrates. In addition to being structurally similar to helicases, SecA is functionally related to the hexameric AAA ATPases which contain six or twelve RecA-like NBDs, such as p97, Clp proteins, and mitochondrial YME1 (23). These AAA ATPases translocate polypeptide substrates through their central pores (24–27). During ATP hydrolysis, the pore loops from each ATPase subunit cooperate to form a dynamic stairway conformation so that the polypeptide substrate is passed from one loop to another in a "hand-over-hand" fashion (28). Despite structural and functional similarities, it is unclear whether SecA uses mechanisms similar to those of helicases or AAA ATPases for substrate translocation.

Author contributions: L.D., S.Y., C.S., and L.L. designed research; L.D., S.Y., J.C., X.W., D.S., C.S., and L.L. performed research; L.D., S.Y., C.S., and L.L. contributed new reagents/analytic tools; L.D., S.Y., C.S., and L.L. analyzed data; and L.D., S.Y., C.S., and L.L. wrote the paper.

The authors declare no competing interest.

This article is a PNAS Direct Submission.

[1]Present address: Institute of Animal Sciences, Chinese Academy of Agricultural Sciences, Beijing 100193, China.

[2]To whom correspondence may be addressed. Email: c.song@pku.edu.cn or long_li@pku.edu.cn.

This article contains supporting information online at https://www.pnas.org/lookup/suppl/doi:10.1073/pnas.2208070120/-/DCSupplemental.

Published January 4, 2023.

Indeed, the NBDs of SecA are unlikely to move along the polypeptide substrates in an inchworm motion as the NBDs do not contact the polypeptides directly like those of helicases with their DNA/RNA substrates (17). Similarly, the "hand-over-hand" model of AAA ATPases cannot be simply applied to SecA because SecA is monomeric when complexed with the SecY channel (15).

The working mechanism of SecA-mediated protein translocation is disputed. In a diffusion-based "Brownian ratchet" model (29, 30), SecA acts as a regulatory protein whose THF senses the sizes of residues in the polypeptide substrates. When the THF encounters residues with large side chains, SecA converts to the ATP-bound state to open up the SecY channel, allowing the residues to pass through the central pore (*SI Appendix*, Fig. S1*B*). After ATP hydrolysis, the channel is reclosed. In a "push–slide" model (31–33), SecA acts as an active motor instead of as a passive regulator suggested by the Brownian ratchet model. The THF is proposed to act similarly to the pore loops of the AAA ATPases, which interact and move the polypeptide substrates directly. Although SecA only has one THF, the clamp has been suggested to cooperate with the THF. Upon ATP binding, the THF makes direct contacts with the polypeptide substrate and pushes the polypeptide toward the channel. As ATP hydrolyzes, the THF retracts, and the clamp holds the polypeptide chain tightly, so that the polypeptide is not dragged backward when the THF resets.

The ambiguity of the translocation mechanism is largely due to the lack of some key intermediate structures during protein translocation. The crystal structures of SecA alone have been determined in the apo state, ADP-bound state, and ATP-bound state (13, 34, 35). However, few conformational changes were observed in the structures upon binding of the nucleotides, thus providing limited mechanistic insight on substrate translocation. The structures of the SecA–SecY translocation complexes have been determined only in the presence of ADP·BeF_3^-, a nonhydrolyzable ATP mimic that promotes tight binding of SecA to SecY (15). The complex structures in other nucleotide-bound states, particularly the ADP-bound state, are highly desired for understanding the coupling mechanism of ATP hydrolysis and protein translocation. These intermediate structures are expected to reveal how the THF may sense the sizes of the substrate residues according to the Brownian ratchet model, and/or if the THF may undergo large conformational changes to drive the polypeptide substrates as predicted by the push–slide model. However, the weak affinity between SecA and SecY after ATP hydrolysis has been the major hindrance to obtaining those structures (31, 36, 37). To overcome the problem, the SecA–SecY complex with a polypeptide substrate was stabilized by reversible cross-linking and cleavable protein fusion during purification in detergent. The cross-linking and protein fusion restraints were released only after the complex had been reconstituted into lipid nanodiscs, which mimicked the native membrane environment and stabilized the complex in vitro (38). The unrestrained polypeptide represented the translocating substrate in the pathway. With this strategy, we determined the cryo-EM structures of the SecA–SecY complex with a translocating polypeptide substrate in the ADP·BeF_3^- bound state and the ADP-bound state. The structures reveal the critical role of the clamp in moving the polypeptide substrates. As nucleotide-binding changes, SecA and the polypeptide substrate undergo similar conformational changes to those of the helicases and their nucleic acid substrates. The movements of the polypeptide substrates in the SecA–SecY complex during posttranslational translocation share a similar structural basis to those in the ribosome–channel complex during cotranslational translocation.

Results

Capture of Translocation Intermediates. On the basis of previous structural studies (16, 17), a translocation complex was designed to contain *Bacillus subtilis* SecA (residues 1 to 778), *Geobacillus thermodenitrificans* SecYE, and a polypeptide substrate. The substrate consisted of the N-terminal signal sequence of OmpA (proOmpA), a short peptide, and a C-terminal superfolder GFP (sfGFP) (39). To allow better resolution of the substrate segment captured in SecA, four tyrosine residues (4Y, residues 50 to 53) flanked by serine and glycine residues were introduced in the short peptide between the signal sequence and sfGFP, resulting in the substrate proOmpA_{4Y}–sfGFP (*SI Appendix*, Fig. S2*A*). Although the introduced Y residues are bulky, the 4Y sequence is unlikely to arrest protein translocation as substrates with the 4Y mutation could be translocated by SecA efficiently (*SI Appendix*, Fig. S2*B*). In addition, four consecutive aromatic residues, including phenylalanine (F), tyrosine (Y), and tryptophan (W), are also observed in the natural substrates of SecA, such as LamB (residues 142 to 145, FYYW). To stabilize GFP in the complex during purification, a GFP nanobody (enhancer) and a 3C cleavage site were fused to the C terminus of SecA. To stabilize the substrate in the channel, residue 29 in the substrate was mutated to cysteine, which was capable of forming a disulfide bond with a cysteine (60C) in the plug of SecY (*SI Appendix*, Figs. S1*B* and S2*C*). The translocation complex was assembled in *Escherichia coli* cells by coexpression of the individual components, after which the complex was purified and reconstituted into lipid nanodiscs. Once the substrate was stabilized in the lipid membrane environment, its restraints were removed by cleavage of the 3C site to free sfGFP and enhancer from SecA, as well as by breakage of the disulfide bond with DTT to free the polypeptide substrate in the channel (*SI Appendix*, Fig. S2*D*). The resulting active translocation complex exists in a lipid environment and contains a polypeptide substrate with the freedom to move in the translocation pathway (38) (*SI Appendix*, Fig. S2 *E–G*).

The translocation complex was incubated with ADP·BeF_3^-, an ATP analog or ADP for cryo-EM single particle analysis (*SI Appendix*, Figs. S3 and S4). The structure with ADP·BeF_3^- was determined to 3.35 Å resolution, the highest resolution so far for the SecA–SecY complexes with ADP·BeF_3^-. More importantly, the structure with ADP was obtained and was determined to be 3.33 Å. Most regions of the maps for SecA have a local resolution better than 3 Å, which enables accurate assignment of the residues in the structures (*SI Appendix*, Figs. S3*C*, S4*C*, and S5 *A–J*). ADP and Mg^{2+} are well resolved in both density maps. BeF_3^- is less resolved in the density map of the complex with ADP·BeF_3^-; however, structural analysis (see below) suggests that most likely BeF_3^- and ADP have been captured together. In both structures, one SecA molecule docks on one SecYE channel and lies approximately parallel to the membrane (Fig. 1 *A* and *B*). NBD1, NBD2, PPXD, and HWD are positioned clockwise at each corner of a rectangle (Fig. 1 *C* and *D*). The TMs of SecY and the signal sequence are well resolved in the membrane (*SI Appendix*, Fig. S5 *K–P*). The density of GFP and enhancer is poor, consistent with their high mobility after 3C protease cleavage.

Conformational Changes of the Nucleotide-Binding Site. SecA has two RecA-like nucleotide-binding domains, NBD1 and NBD2. Large movements are observed for the two domains when comparing the ADP·BeF_3^-–bound state and ADP-bound state (Fig. 1 *C* and *D*). In the structure with ADP·BeF_3^-, NBD1 and NBD2 are in a "closed" conformation, same as the conformations of NBD1 and NBD2 in the available SecA–SecY structures with

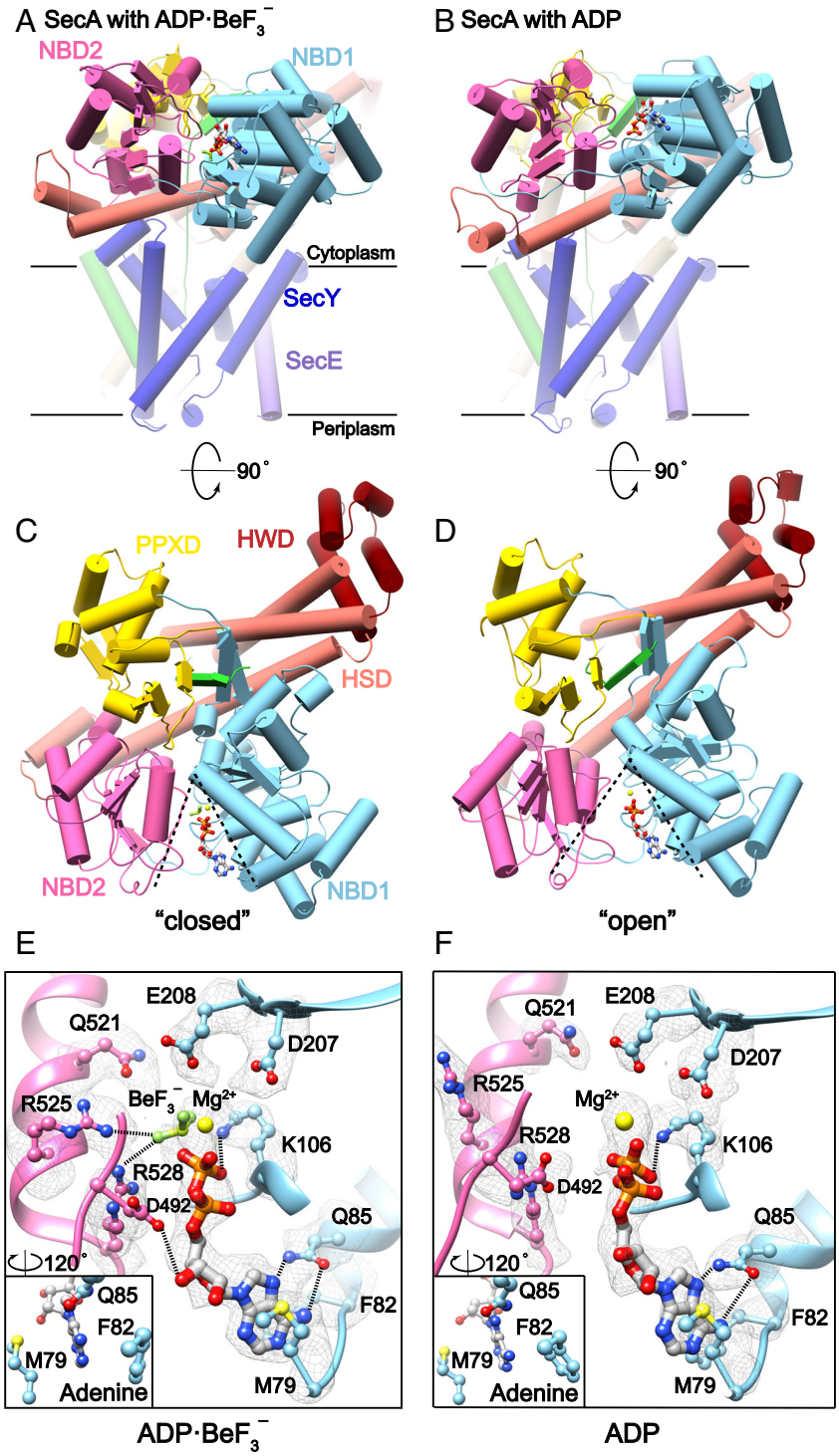

Fig. 1. Structures of the SecA/SecYE/proOmpA$_{4Y}$–sfGFP complex in the ADP·BeF_3^- and ADP-bound states. (*A*) Cylinder model of the ADP·BeF_3^--bound structure. Individual domains and proteins are colored as follows: *Bacillus subtilis* (*Bs*.) SecA NBD1, sky blue; NBD2, hot pink; PPXD, yellow; HSD, salmon; HWD, dark red; *G. thermodenitrificans* (*Gt*.) SecE, purple; N-half of SecY, medium blue; C-half of SecY, tan; and proOmpA$_{4Y}$, lime green. The nucleotide is shown as balls and sticks. (*B*) Cylinder model of the ADP-bound structure. Individual domains and proteins are colored as in *A*. (*C*) Top view of *A*. The opening of the nucleotide-binding site is defined by the dashed line connecting residues E131 and D492 on the left side and the other dashed line connecting residues E131 and K106 on the right side. The residues are not marked in the figure for a clearer view. (*D*) Top view of *B*. The opening of the nucleotide-binding site is indicated as in *C*. (*E*) Coordination of ADP·BeF_3^- in the nucleotide-binding site. The hydrogen bonds between the nucleotide and the residues from SecA are indicated by dashed lines. The residues and nucleotide are shown as balls and sticks with density in mesh. The carbon atoms from NBD1 and NBD2 are colored sky blue and hot pink, respectively. The nitrogen, oxygen, phosphorus, and magnesium atoms are colored blue, red, orange, and yellow, respectively. BeF_3^- is colored green. The sandwich arrangement of adenine, M79, and F82 is viewed at a rotation of 120° in the inset. (*F*) Coordination of ADP in the nucleotide-binding site. The color scheme is the same as that in *E*.

ADP·BeF_3^- (*SI Appendix*, Fig. S6 *A–C*) (15–17). However, the higher resolution of the structure reported here allows us to examine nucleotide binding in detail. ADP·BeF_3^- is held between the two domains (Fig. 1*E*). Adenine is sandwiched between M79 and F82 in NBD1. Q85 of NBD1 further stabilizes adenine via two hydrogen bonds. The 3′-OH of the ribose is hydrogen-bonded to D492 of NBD2. The Walker A motif (T102–T107) of NBD1 interacts with the diphosphate moiety. In particular,

the β-phosphate is hydrogen-bonded to NH of K106. D207 and E208 of the Walker B motif (V205–D210) coordinate with Mg^{2+}. BeF_3^- mimics the γ-phosphate and is coordinated from the side by R528 and arginine finger R525 from NBD2. Q521 is in the position ready for orientating the catalytic water, which is not well resolved in the density map, however (20). The importance of these residues in ATP binding has been confirmed by previous mutagenesis studies (40). In the structure with ADP, NBD1 binds to ADP and Mg^{2+} in the same mode as that in the structure with ADP·BeF_3^- (Fig. 1*F*). However, without BeF_3^-, the side chains of polar residues Q521, R525, and R528 of NDB2 all point away from ADP. The hydrogen bond between D492 and ribose is also disrupted. Thus, NBD2 is no longer involved in nucleotide binding. As a result, NBD2 and NDB1 move away from each other, resulting in an "open" conformation. The changes between the open and closed conformations upon binding of different nucleotides are not observed in the crystal structures of SecA alone. In the previous crystal structures (13, 34, 35), NBD1 and NBD2 are in their open conformations regardless of ATP or ADP binding (*SI Appendix*, Fig. S6 *D–F*). On the other hand, the nucleotide-binding modes of the two NBD domains in the translocation complex are highly similar to those of helicases. The NBDs of the helicases are in an open conformation in the apo state and are closed upon binding of the ATP analogs when complexed with their DNA/RNA substrates (19, 20) (*SI Appendix*, Fig. S6 *G* and *H*). The residues involved in ATP/ADP binding are conserved among SecA and the helicases (*SI Appendix*, Figs. S6*I* and S7 *A–E*). Besides the Walker A and Walker B motifs shared in the RecA-like ATPase family, D492 and R525 of NBD2 in SecA, which directly interact with nucleotides, are also highly conserved.

Domain Movements of SecA in the Two States. SecA undergoes global conformational changes between the ADP·BeF_3^- and ADP states due to the closure and opening of the nucleotide-binding site. Taking SecY and the membrane as references, superimposition of the two structures shows that the largest movements are seen at NBD1 and NBD2 (Fig. 2*A*). The central β-sheet of NBD2 has a slight upward shift, moving 2 Å away from the membrane in the ADP·BeF_3^- structure when compared with the ADP structure, whereas the peripheral α-helices have a clockwise rotation of ~20° when viewed from the side. With ADP·BeF_3^-, NBD1 has a significant downward shift of 7 Å toward the membrane while moving closer to NBD2. Other domains have local, but significant, conformational changes. The long α-helix of HSD, which spans the entire SecA molecule, has a displacement of 15 Å at the end close to NBD2 (Fig. 2*B*). In contrast, the THF in HSD is essentially the same in the two structures (Fig. 2*C*). The largest movement in PPXD is seen in a loop of PPXD (residues 314 to 325, C loop) that reaches a cavity between NBD1 and NBD2 opposite to the nucleotide-binding site (Fig. 2 *C* and *D*). The C loop, which cooperates with NBD2, has an inward and upward shift, moving away from the membrane in the ADP·BeF_3^- state. HWD in the ADP·BeF_3^- structure has a small shift, moving ~3 Å away from the membrane (Fig. 2*C*).

SecY and its Interactions with SecA in the Two States. The SecY channel has few changes between the two structures, with a r.m.s.d. of 0.79 Å (Fig. 2 *A* and *C*). The interactions between the C-half of SecY and SecA are also largely unchanged. PPXD sits on the loop between TM8 and TM9 (L8/9) of SecY (Fig. 2*E*). The THF inserts into the cleft between TM8 and TM10 on the cytoplasmic side. The major interaction changes are between SecA and the N-half of SecY, particularly the long α-helix of HSD and L2/3 of SecY (Fig. 2*B*). In the presence of ADP, the long α-helix and L2/3 are positioned away from each other, whereas in the ADP·BeF_3^- structure, due to the large displacement of the long α-helix, the long α-helix is positioned directly on top of L2/3. As a result, SecA has major interactions only with the C-half of SecY in the ADP structure, whereas SecA interacts with both the N-half and C-half of SecY in the ADP·BeF_3^- structure. Consistently, SecA has a much lower affinity to SecY in the ADP state or apo state than in the ATP state (31, 36, 37). The dynamic interactions between the long α-helix and NBD1 and NBD2 have been shown to be critical for protein translocation as they allow the motions of NBD1 and NBD2 to be transferred to the long α-helix during ATP hydrolysis (41).

Polypeptide Substrate in the Translocation Complex. The N-terminal signal sequence at the lateral gate and the following polypeptide in the channel are essentially the same in the ADP and ADP·BeF_3^- structures (*SI Appendix*, Fig. S8 *A* and *B*). Residue G31 is locked at the pore ring (*SI Appendix*, Fig. S8 *B* and *C*). The density of the polypeptide substrates becomes weak in proximity to the THF of SecA (*SI Appendix*, Fig. S8 *D* and *E*). Nevertheless, it is clear that, in both structures, at the tip of the THF, the side chain density of the highly conserved Y743 and the weak density of the polypeptide are connected (*SI Appendix*, Fig. S8 *F* and *G*). This finding suggests that, although the substrate is not held in a fixed position as it enters the channel, it could interact with the THF, particularly with Y743, which has been suggested to be important for protein translocation (31, 33, 42). The substrate segment in SecA immediately before the contact point with the THF is untraceable in the density map, indicating that the segment is disordered. Indeed, along the translocation pathway, the space between the clamp and pore ring of SecY is relatively open, allowing considerable flexibility of the polypeptides in the unfolded states, which are required for the substrates to pass through the central pore of the channel (43).

The density of the following polypeptide substrate in the clamp of SecA is well resolved (Fig. 3 *A* and *B*). The side chains of the four consecutive tyrosine residues (Y50–Y53) can be unambiguously assigned in the polypeptide segment (Fig. 3 *C* and *D*). In both structures, the polypeptide is sandwiched as a β-strand by the TCβ on one side and the PP loop of PPXD on the other side similar to the previous structure (17). The aromatic rings of Y50 and Y52 point in the opposite direction as those of Y51 and Y53 (Fig. 3 *C* and *D*). However, it is clear that the clamped polypeptide has different conformations in the ADP·BeF_3^- and ADP states. In the ADP·BeF_3^- structure, the main chain of the TCβ forms three hydrogen bonds with residues 52 to 54 of the polypeptide substrate, whereas the PP loop forms three hydrogen bonds with residues 49 to 51 (Fig. 3*E*). The side chain of R327 from the PP loop inserts between Y50 and Y52. Y52 forms a π–π interaction with F182 from NBD1 (Fig. 3*C*). In the ADP structure, residues 50 to 51 of the substrate join residues 52 to 54 to form an extended β-strand, which has five hydrogen bonds with the TCβ (Fig. 3*F*). The PP loop keeps the same three hydrogen bonds as it does in the ADP·BeF_3^- structure but with residues 47 to 49 of the polypeptide substrate (Fig. 3*F*). For the side chain interactions, instead of R327, now F182 of NBD1 inserts between Y50 and Y52 (Fig. 3*D*). R327 in the structure is now in contact with S48. Y50 forms an amino–π interaction with N178 of NBD1, whereas Y52 forms a cation–π interaction with R186 of NBD1. The residues N178, F182, and R186, which interact with the substrate via side chain interactions, are all located on one face of a short α-helix in NBD1 (residues 176 to 189, α8).

Extensive hydrogen bonds have also been observed between the helicases and their nucleic acid substrates (19–21), as well

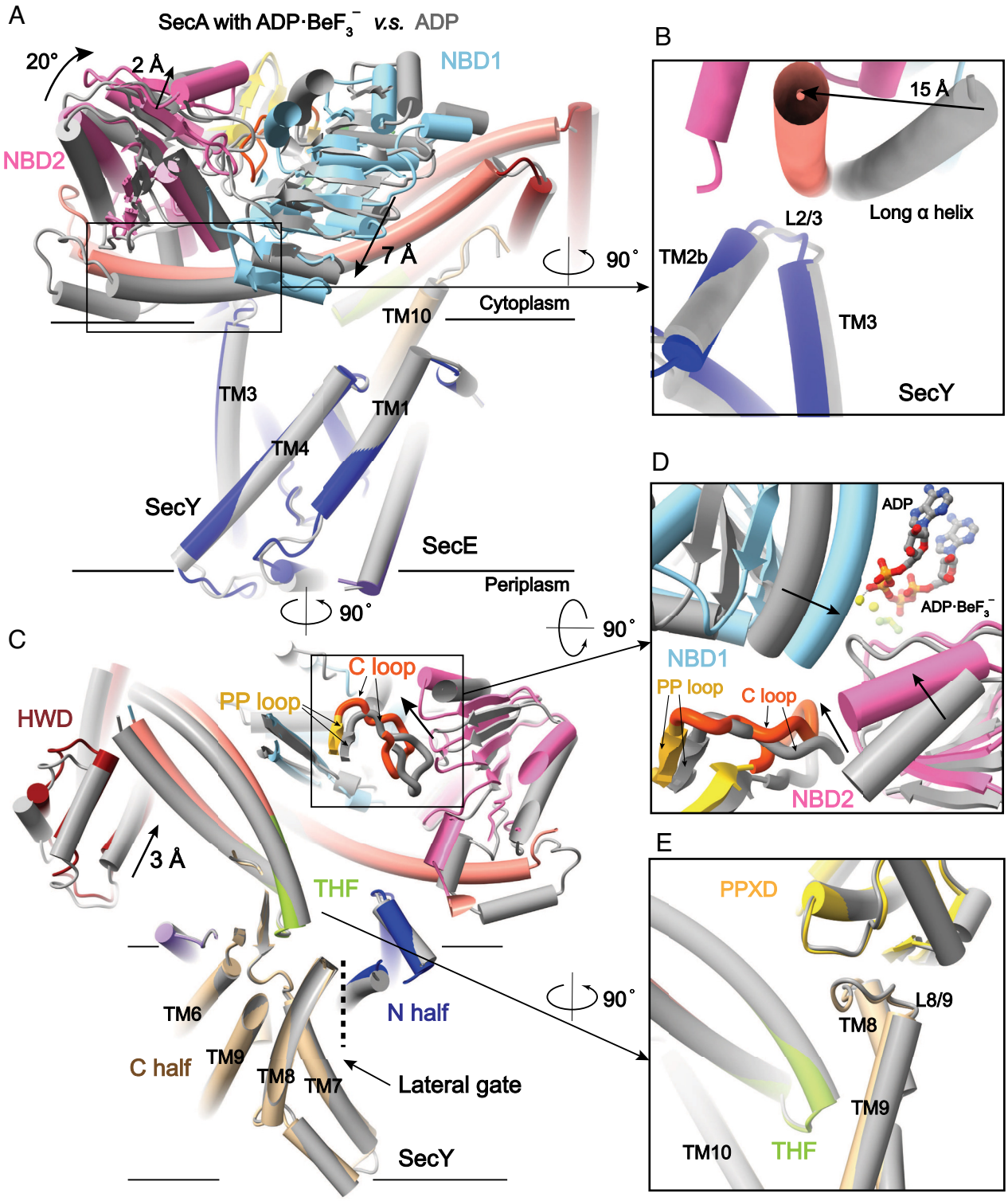

Fig. 2. Comparison of SecA and SecY in the ADP·BeF_3^--bound and ADP-bound structures. (*A*) Superimposition of the ADP·BeF_3^--bound and ADP-bound structures using SecY as the reference. The color codes of the ADP·BeF_3^--bound structure are the same as those in Fig. 1*A*. The ADP-bound structure is colored gray. The motions of NBD2 and NBD1 in the two structures are indicated with arrows. (*B*) A close-up view of the long α-helix in HSD and L2/3 of SecY. The long α-helix is colored salmon in the ADP·BeF_3^- structure and colored gray in the ADP structure. The motion of the long α-helix in the two structures is indicated by an arrow. L2/3 is colored medium blue in the ADP·BeF_3^- structure and colored gray in the ADP structure. (*C*) As in A, but from a view rotated by 90°. The C loop, PP loop, and THF from the ADP·BeF_3^- structure are highlighted in orange, gold, and green, respectively. The ADP structure is colored gray. (*D*) *Top* view of the C loop in the ADP·BeF_3^- and ADP structures. The coloring is the same as that in *C*. The motions of NBD1, NBD2, and the C loop upon ADP·BeF_3^- binding are indicated by arrows. (*E*) Interactions of SecA and the C-half of SecY, including L8/9 of SecY, PPXD of SecA, and the THF. Individual domains and TMs are labeled and colored as in *A*.

as between the AAA ATPases and their polypeptide substrates (27, 44, 45). Interestingly, in all three cases, the residues, usually aromatic amino acids, from the ATPases intercalate between the side chains of the polypeptide substrates or between the nucleobases of nucleic acid substrates (19, 27) (*SI Appendix*, Fig. S9).

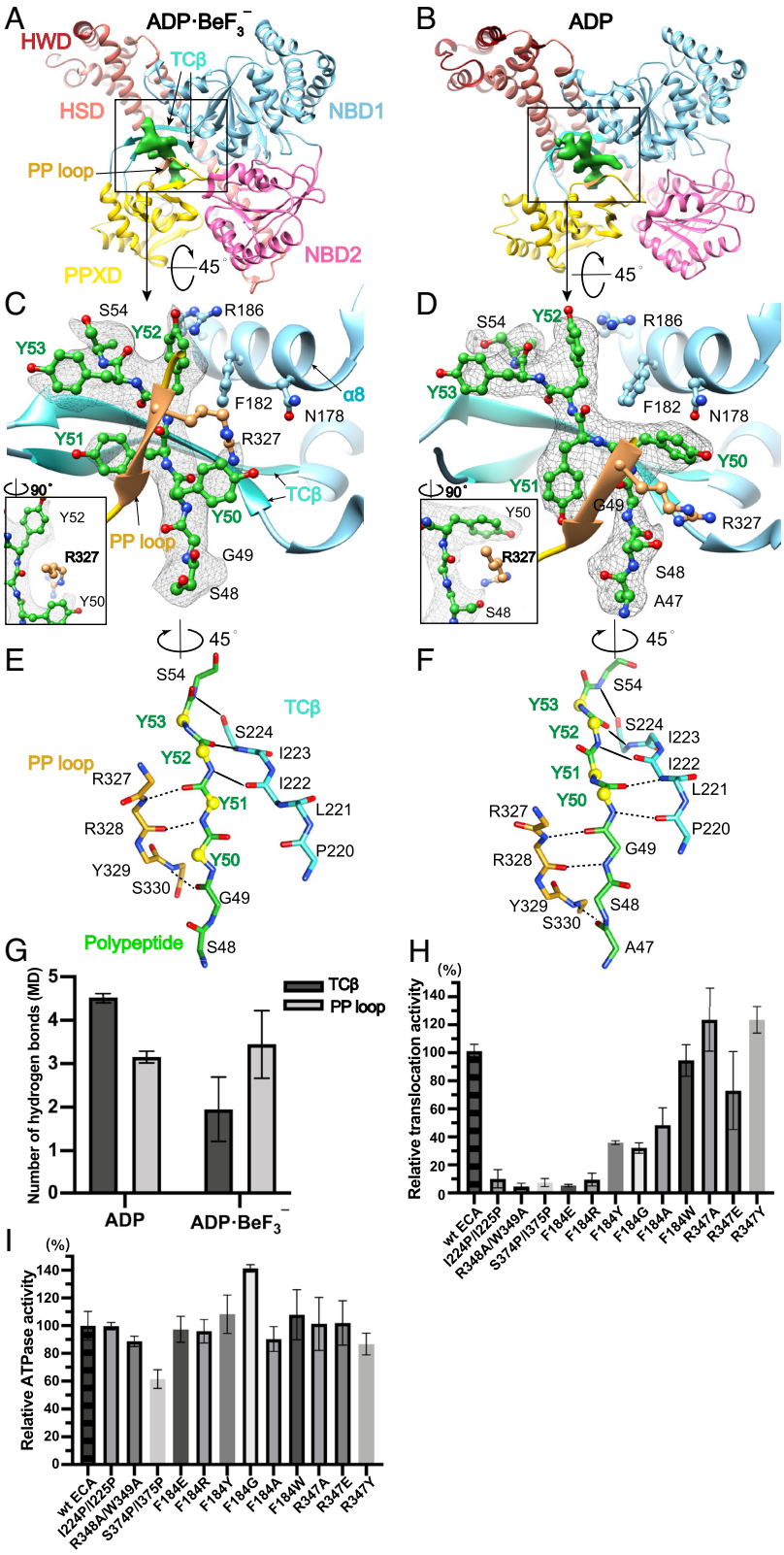

Fig. 3. Interactions between the clamp of SecA and the polypeptide substrate. (*A*) Top view of the ADP·BeF_3^- structure showing polypeptide entry into SecA. Individual domains are colored as in Fig. 1*A*. The polypeptide substrate is shown as green density. (*B*) Top view of the ADP structure, the same view as in *A*. (*C*) The polypeptide substrate in the clamp in the ADP·BeF_3^- structure. The substrate, including the four consecutive tyrosine residues, is shown as balls and sticks with the cryo-EM density as a gray mesh. The TCβ, PP loop, and α8 of SecA are labeled and shown as ribbons with the side chains shown as balls and sticks. The intercalation of R327 into the substrate is presented in the *Inset*. (*D*) The polypeptide substrate in the clamp in the ADP-bound structure. (*E*) The main chain interactions between the substrate and the clamp in the ADP·BeF_3^- structure. The hydrogen bonds are indicated by dashed lines. The hydrogen bonds unchanged in the ADP·BeF_3^- and ADP structures are shown as solid lines. The Cα of the four Y residues are highlighted as yellow balls. (*F*) The main chain interactions between the substrate and the clamp in the ADP structure. (*G*) The main chain interactions between the substrate and the clamp in the ADP·BeF_3^- and ADP states from MD simulations. Shown are the hydrogen bond numbers between the main chains of the polypeptide substrate and the TCβ or PP loop from the last 500-ns trajectories of multiple 1-μs MD simulations. The means and SDs were calculated on the basis of three independent simulations of each state. (*H*) The relative translocation activities of the SecA mutants compared with wild-type SecA. The means and SDs were calculated using the average values of the results from at least three experiments. (*I*) The relative ATPase activities of the SecA mutants compared with wild-type SecA.

Interactions between the Clamp and the Substrate Controlling Protein Translocation. The interactions between the main chains of the polypeptide substrates and SecA likely play critical roles in protein translocation because SecA moves polypeptides without sequence specificity. In the ADP state, TCβ forms five hydrogen bonds with the main chain of the polypeptide substrate on one side, while the P loop forms three hydrogen bonds with the main chain of the polypeptide substrate on the other side (Fig. 3*F*). In the ADP·BeF_3^- structure, the number of hydrogen bonds between TCβ and the polypeptide is reduced to three, and the hydrogen bond number of the PP loop remains unchanged (Fig. 3*E*). To further quantitatively analyze the dynamic binding of the clamp to the polypeptide in the main chains, we performed all-atom molecular dynamics (MD) simulations based on the ADP and ADP·BeF_3^- structures (*SI Appendix*, Fig. S10 *A* and *B*). During multiple 1-μs simulations in the ADP state, the main chains of the TCβ consistently formed more hydrogen bonds with the substrate in comparison with the PP loop (average of ~ 4.5 vs. ~3.2), whereas the number of hydrogen bonds mediated by the TCβ was fewer than that mediated by the PP loop in the ATP state (average of ~2.0 vs. ~3.4) (Fig. 3*G* and *SI Appendix*, Fig. S10 *C*–*F*). This result suggested that the relative binding strength of the TCβ and PP loop to the substrate alternates in the ADP and ATP states, as measured by the number of stably formed hydrogen bonds. Similarly, in the helicase structures, the strength of binding between the two NBDs and the nucleic acid substrates alternates between different nucleotide-binding states (22).

To verify the importance of the main chain interactions during protein translocation, the highly conserved residues of the TCβ and PP loop involved in substrate interactions were selected for mutagenesis studies. The corresponding residues in *Escherichia coli* SecA were mutated, and the translocation activities of the mutants were examined. Proline residues were introduced to disrupt hydrogen bonding between the main chains. I224P/I225P (I222P/I223P in *Bacillus subtilis* SecA) in one β connecting peptide of the TCβ, S374P/I375P (T354P/I355P in *Bacillus subtilis* SecA) in the other β connecting peptide, and R348P/W349P (R328/Y329P in *Bacillus subtilis* SecA) in the PP loop all abolished the translocation activity of SecA (Fig. 3*H* and *SI Appendix*, Fig. S11*A*), while the ATPase activity levels of the mutants were largely unaffected (Fig. 3*I*). These results confirmed the critical roles of clamping and β-strand formation during translocation.

The extensive side chain interactions between SecA and the polypeptide substrates in the structures indicate that they may also be important in mediating protein translocation. Structural comparison of the substrate in the clamp suggests that two residues are particularly interesting, F182 in the middle of α8 in NBD1 and R327 in the PP loop. F182 intercalates between Y50 and Y52 of the substrate in the ADP state, while it forms a π–π interaction with Y52 in the ADP·BeF_3^- structure (Fig. 3 *C* and *D*). F182 is completely conserved among different species (*SI Appendix*, Fig. S11*B*). We mutated the corresponding F184 in *Escherichia coli* SecA into several different amino acids without affecting the ATPase activities (Fig. 3*I*). Most mutants had severe defects in translocation with the exception of F184W (Fig. 3*H*). In particular, mutation of F184 into Arg (F184R) or Glu (F184E) dramatically decreased the translocation activity of SecA (Fig. 3*H* and *SI Appendix*, Fig. S11*C*), highlighting the importance of side chain interactions in protein translocation. R327 has substrate-binding modes similar to those of F182 but from the opposite side in the PP loop (Fig. 3 *C* and *D*). The side chain of R327 intercalates between Y50 and Y52 in the ADP·BeF_3^- structure, while it points to S48 in the ADP structure. In contrast to F182, mutation of the highly conserved R327 equivalent in *Escherichia coli* SecA, R347, to other amino acids did not seem to greatly affect the translocation activity of SecA (Fig. 3*H* and *SI Appendix*, Fig. S11 *D* and *E*). These data highlighted the important role of side chain interactions mediated by aromatic residues during protein translocation by SecA. Similarly, the aromatic residues in the pore loops are critical for protein translocation by AAA ATPases (28). These residues intercalate in the polypeptide substrates and have been suggested to drive the substrate through the central pore of the hexameric assembly of AAA ATPases during ATP hydrolysis (*SI Appendix*, Fig. S9 *B* and *E*).

Motions of the Polypeptide Substrate and the Clamp. With the help of the four Y residues in the substrates, we precisely traced the movement of the substrate in the clamp upon ATP binding (mimicked by ADP·BeF_3^-). Compared with the structure with ADP, all four tyrosine residues in the ADP·BeF_3^- structure have a shift of ~4 Å into SecA toward SecY and the membrane (Fig. 4 *A* and *B*). In the same direction, the TCβ that has the hydrogen bonds with the main chain of the substrate moves ~4 Å toward the membrane as well. The hydrogen bonds between the main chains of I222 and S224 from the TCβ and Y51–Y52 from the substrate are unchanged (Fig. 3 *E* and *F*). α8 of NBD1, which interacts with the four Y residues via the side chains, also has a shift of 3.5 to 4.0 Å toward the membrane (Fig. 4*B*). The movements of the TCβ and α8 are both due to the movement of NBD1 as a rigid body upon ADP·BeF_3^- binding. In contrast, the PP loop on the other side of the substrate has an opposite shift, moving ~3 Å away from the membrane (Fig. 4*C*). The opposite shift is due to the movement of the preceding C loop, which is pushed up and away from the membrane when NBD1 and NBD2 move close to each other upon ADP·BeF_3^- binding (Fig. 2 *C* and *D*). The immediate result of the opposite shift between the PP loop and the substrate is that the H-bonding of the PP loop to S48–G49 of the polypeptide in the ADP state is changed to Y50–Y51 in the ATP-binding state (Fig. 3 *E* and *F*).

The motions of the polypeptide substrates in the clamp are highly similar to those of the nucleic acid substrates in helicases (19–21). Upon binding of ATP analogs, the closing of the RecA-like domains 1A and 2A (equivalent to NBD1 and NBD2) in the helicases leads to a relative shift of the substrate by one nucleotide (*SI Appendix*, Fig. S9 *A* and *C*). Domains 1A and 2A interact with nucleic acids directly in the process. Similarly, one residue of the polypeptide is shifted in the clamp of SecA upon binding of ATP analogs, although in this case, NBD1 and NBD2 do not directly interact with the polypeptide substrates. The movements of NBD1 and NBD2 upon closing are transferred to the TCβ and the PP loop to drive the movement of the polypeptide (*SI Appendix*, Fig. S9*D*).

Engaging the Polypeptide Substrates in the Clamp. Peptide binding in the clamp region has also been observed in the crystal structures of SecA alone (13, 46). A peptide segment of the C-terminal tail joins the β-sheet with the TCβ in full-length SecA (*SI Appendix*, Fig. S12*A*). In a crystal structure of the C-terminal truncated SecA, a peptide segment from the neighboring SecA molecule is paired with the TCβ (*SI Appendix*, Fig. S12*B*). In both crystal structures, the peptide segments adopt conformations more similar to the conformation of the polypeptide substrate in the clamp in the ADP state than in the ATP state (*SI Appendix*, Fig. S12 *C* and *D*). NBD1 and NBD2 are in the open conformation, and PPXD is not in proximity to the TCβ to form the clamp in the crystal structures (*SI Appendix*, Fig. S12 *A* and *B*). Thus, the TCβ alone is sufficient to induce the β-conformation of the polypeptides. The PP loop on the other side of the polypeptides likely controls the running direction of the substrates as β-strands of the substrate are bent where the PP loop interacts in the ADP and ADP·BeF_3^- structures (Fig. 4 *B* and *C*).

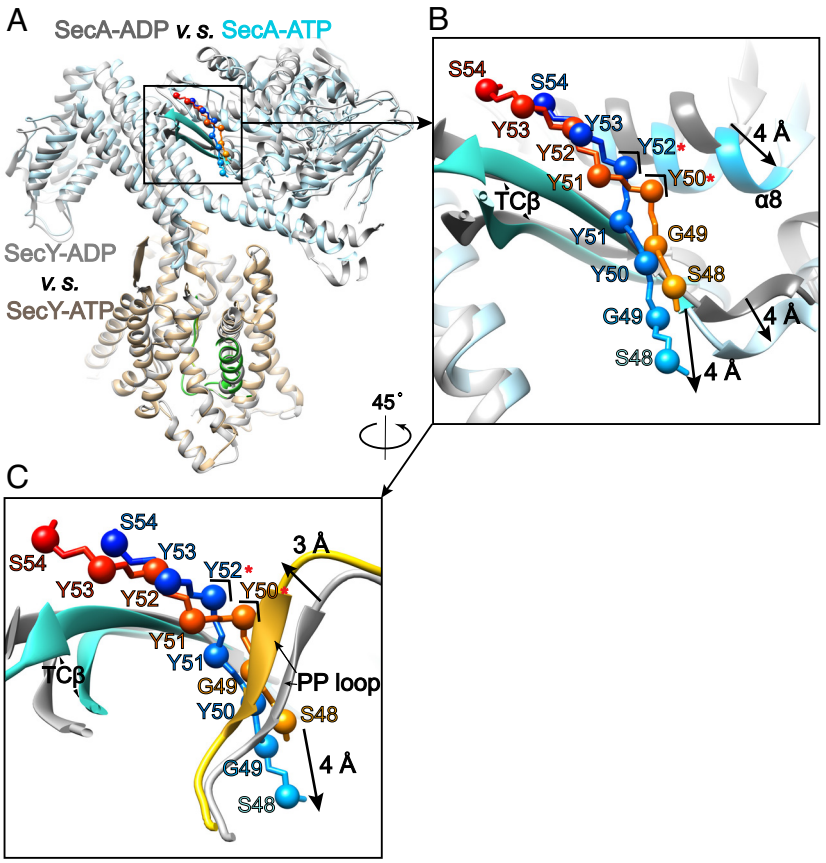

Fig. 4. Movements of the polypeptide substrate and clamp. (*A*) Superimposition of the ADP and ADP·BeF_3^- structures using SecY as the reference. SecA, SecY, and the signal sequence in the ADP·BeF_3^- structure are colored cyan, tan, and lime green, respectively. The ADP structure is colored gray. (*B*) A close-up view of the clamp and the substrate in the ADP and ADP·BeF_3^- structures. The TCβ and α8 are labeled. The main chains of the polypeptide substrate are labeled and shown as sticks with Cα as balls. The polypeptide in the ADP structure is colored light red (N terminus) to dark red (C terminus). The polypeptide in the ADP·BeF_3^- structure is colored light blue (N terminus) to dark blue (C terminus). The movements of the TCβ, α8, and substrate are indicated by arrows. The bending points of the polypeptide substrate are indicated with corners, and the residue labels are marked with red *. (*C*) as in *B*, but from a different angle to show the PP loop. The motion of the PP loop is indicated by an arrow.

Comparison of NBD1, NBD2, and PPXD in different structures reveals how polypeptide substrates may be engaged in the clamp for translocation. In SecA alone, the clamp is not formed because the PPXD is flexible (35, 47). The TCβ alone may be sufficient to recruit the substrate to the clamping site without the PP loop from PPXD (*SI Appendix*, Fig. S12*E*). When complexed with the SecY channel, PPXD undergoes a large fold-back rotation to dock on the channel (15) (Fig. 2*E*). The "fold-back" conformation presents the C loop to the cavity between NBD1 and NBD2 in a position that allows the C loop and the PP loop to undergo conformational changes following the opening and closing of NBD1 and NBD2 during ATP hydrolysis (Fig. 2*D*). More importantly, in the fold-back conformation, the clamp is formed by the PP loop and the TCβ with the prepositioned polypeptide substrate being fully engaged in between (*SI Appendix*, Fig. S12*F*). The importance of the C loop in clamp formation and protein translocation is supported by a previous study showing that mutations of highly conserved R322 in the C loop disrupted its interactions with NBD1 and NBD2 and abolished protein translocation (48) (*SI Appendix*, Fig. S11*D*).

Discussion

"Hand-Switching" Model of Polypeptide Movement by the Clamp. The similarity in substrate binding between SecA and helicases indicates that they may use similar mechanisms for moving their substrates. Structures (49) and molecular simulations (50) of helicases show that the relative binding strength of NBDs to substrates is changed by shifting from the ADP/apo state to the ATP state. The alternation of the interaction strength coupled with the opening and closing of NBDs during ATP hydrolysis is required for helicases to generate one-direction inchworm motion along nucleic acids (Fig. 5*A*). Similarly, coupled with ATP hydrolysis, the alternation of substrate-binding strength from the two sides of the SecA clamp is able to generate the motion of the polypeptide substrates in one direction (Fig. 5*B*). In the ADP-bound state, the TCβ has stronger interactions with the substrate than the PP loop, as measured by the number of H bonds in the main chains. When ADP is replaced by ATP, which is mimicked by ADP·BeF_3^-, NBD1 moves close to NBD2 and toward the membrane. In the same direction, the substrate moves together with the TCβ of NBD1 due to their tight interactions. The PP loop with weaker substrate interactions does not follow the same moving direction. In the ATP-binding state, the PP loop forms stronger interactions with the substrate. The interaction from the PP loop bends the polypeptide and disrupts the hydrogen bonds between the substrate and the TCβ, resulting in a weaker interaction with the TCβ in the ATP-bound state. As ATP hydrolysis occurs and Pi is released, the PP loop holds the substrate tightly, and the weakly bound TCβ resets back to its conformation in the ADP state. The overall result of these processes is that the polypeptide substrate is moved toward the channel when one ATP molecule is hydrolyzed. The step size may not be one residue per ATP as observed in the structures. Due to the heterogeneity of the side chains and their engagement with the clamp, movements

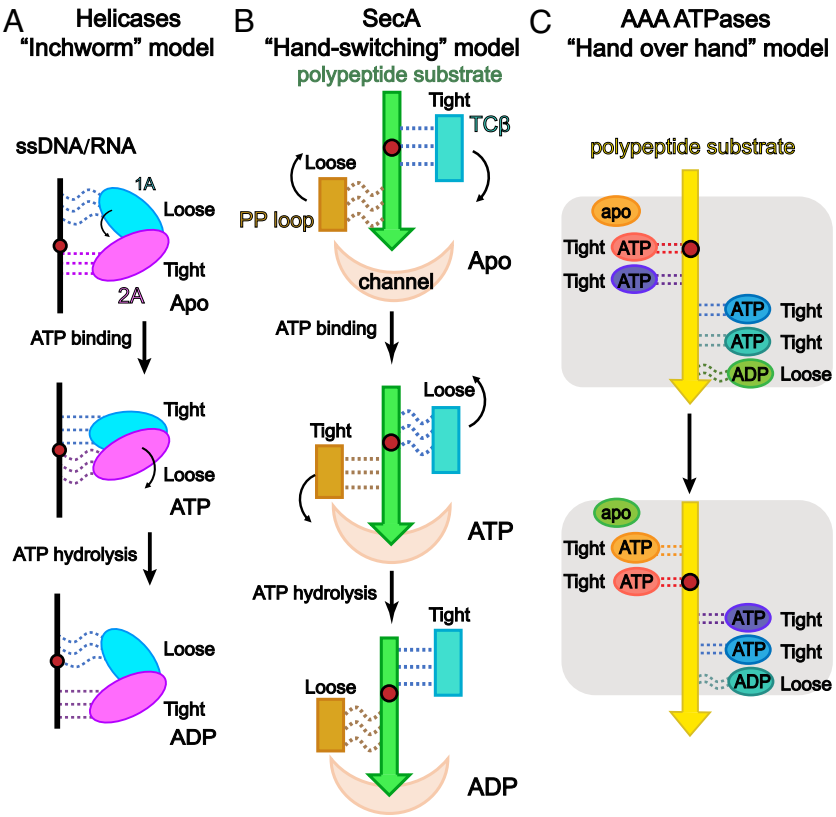

Fig. 5. Translocation mechanisms of helicases, SecA, and AAA ATPases. (*A*) "Inchworm" model of helicases. Single-strand DNA/RNA (ss DNA/RNA) is presented as a black line. The RecA-like domains 1A (deep sky blue oval) and 2A (magenta oval) interact with the substrate. The tight and loose interactions are indicated by straight and crooked dashed lines, respectively. The movements of the domains leading to the next steps are indicated by arrows. The red dot in the substrate serves as a register to indicate the movement of the helicase. Starting from the apo state, helicases translocate along the substrate by one base upon binding and hydrolysis of one ATP molecule. (*B*) "Hand-switching" model of SecA. The TCβ (turquoise rectangle) and PP loop (gold rectangle) interact with the polypeptide substrate (lime green arrow) from two sides. The SecY channel is drawn as a pink crescent. The tight and loose interactions are indicated by straight and crooked dashed lines, respectively. The red dot in the substrate serves as a register to indicate the movement of the polypeptide. The movements of the domains leading to the next steps are indicated by arrows. (*C*) "Hand-over-hand" model of AAA ATPases. The polypeptide substrate (yellow arrow) is surrounded by six RecA-like domains (orange, salmon, middle purple, deep sky blue, dark turquoise, and light green ovals) in a spiral staircase arrangement (transparent gray bar). The nucleotide-binding state of each domain is labeled. The tight and loose interactions are indicated by straight and crooked dashed lines, respectively. The red dot in the substrate serves as a register to indicate the movement of the polypeptide. The cycle begins with the orange domain in the apo state, in which it is not interacting with the substrate. Upon ATP binding, the orange domain on the top is engaged tightly with the substrate. The four preceding ATP-bound domains (salmon, middle purple, deep sky blue, and dark turquoise) progress with the substrate. The light green domain at the bottom releases its ADP and disassociates from the substrate, after which it rotates to the top, back to the apo state, and ready for the next cycle of movement.

of less or more than one residue at the clamp may occur in an ATP hydrolysis cycle (33, 51, 52). Nevertheless, the repetitive motions of the TCβ and PP loop should provide the general motion directionality and push the substrate toward the channel. The movement of the clamp can be considered as a cooperative "hand-switching" motion, in which the substrate is passed from one hand (TCβ) to the other hand (PP loop) to move in one direction. This motion is mechanically similar to the inchworm movement of helicases along their substrates (Fig. 5*A*), as well as to the "hand-over-hand" model for AAA ATPases (Fig. 5*C*), in which the six Rec-like NBDs (hands) have alternative tight and loose interactions with the polypeptide substrates in the presence of different nucleotides. The orchestrated alternation of the interaction strength coupled with the motions of the NBDs enables the passing of the polypeptide substrates between NBDs sequentially, leading to directional movements of the substrates. The tight and loose interactions are mainly controlled by the intercalation states of the aromatic residues from the pore loops of NBDs into the polypeptide substrates in different nucleotide-binding states (*SI Appendix*, Fig. S9 *B* and *E*).

The "hand-switching" model highlights the proactive role of the clamp in moving the polypeptide substrates. SecA acts more likely as a motor driven by ATP hydrolysis than a regulator as suggested by the Brownian ratchet model. The comparison of the ADP and ADP·BeF_3^- structures does not reveal the large conformational changes of the THF as predicted by the "push–slide" model for moving the polypeptide substrates. Instead, the "hand-switching" model proposes that the conformational changes in the clamp alone are likely sufficient to provide the driving force for the polypeptide substrates to move through the SecY channel during ATP hydrolysis.

Motion of Polypeptide Substrates during SecA-Driven Translocation. The driving force from the clamp, however, does not seem to warrant the immediate movement of the polypeptide substrates in the channel. Due to the heterogeneity of the side chains of amino acids, substrates with different sequences may not be pushed by the clamp with equal efficiency. For example, segments rich in residues with bulky side chains, such as the segment containing four Y residues used in our construct, are likely to be tightly coupled with the movement of the clamp, whereas a stretch of residues with small side chains is not likely to be translocated efficiently by the clamp (31). Translocation of these difficult sequences may require Brownian sliding, which is possible in the ADP state. In the ADP-bound structure, the channel has a large degree of freedom to allow free sliding of the polypeptide substrate as SecA only interacts with the C-half of the

channel (*SI Appendix*, Fig. S13*A*). The clamp of SecA alone may not be sufficient to hold the polypeptide substrate tightly. The low affinity between SecA and SecY allows SecA to dissociate from the channel as well (*SI Appendix*, Fig. S13*B*). In line with this model, back-sliding of the substrates from the SecA–SecY complex was observed without nucleotides or with ADP (31, 53).

Upon ATP binding, SecA forms tight interactions with both the N and C halves of the channel (*SI Appendix*, Fig. S13*C*). The substrate is fully engaged in the clamp and the channel. The substrate in the clamp could be pushed forward during ATP hydrolysis cycles (*SI Appendix*, Fig. S13 *A* and *C*). However, the preceding polypeptide in the channel may not follow the same movement immediately because the polypeptide substrates between the clamp and the channel are rather flexible. The polypeptide could accumulate in the space before entering the channel (*SI Appendix*, Fig. S13*D*). After multiple cycles of ATP hydrolysis, the substrate may be forced to move forward eventually as the space available to accommodate the polypeptide before entering the channel is limited (54) (*SI Appendix*, Fig. S13*E*). Protein folding and Brownian diffusion may also play a role in the process (*SI Appendix*, Fig. S13*D*). Particularly, folding of the translocated segments in the extracellular/luminal side could drive translocation of the following polypeptide through the channel (30, 55). Depending on the sequences of the translocating polypeptides, clamp motion, Brownian diffusion, and protein folding may play roles at different stages of protein translocation (30, 51, 52). Nevertheless, the clamp seems to provide the critical directionality of the SecA-mediated translocation because only clamp motion is constantly driven by ATP hydrolysis, whereas both protein folding and Brownian diffusion are spontaneous and highly sequence specific. This scenario is very much similar to cotranslational translocation (8). The nascent chain is highly flexible due to the gap between the peptide exit tunnel of the ribosome and the SecY/Sec61 channel (*SI Appendix*, Fig. S14). The addition of one residue to the nascent chain during translation does not necessarily result in the passing of one residue through the channel. However, continuous elongation of the nascent chain provides the directionality of translocation and drives the substrate through the channel.

During translocation by SecA, the THF may act as a guide point to align the flexible polypeptide to the center of the channel in the ADP-bound and ATP-bound states. This explains the observation that some point mutations of the highly conserved residues in the THF reduced translocation efficiency in vitro (31, 33, 42), while these conserved residues are nonessential (31) and protein translocation still took place when the THF was fixed to the channel by cross-linking (56). Nevertheless, there may be additional conformations of SecA–SecY during ATP hydrolysis. As shown by smFRET, the THF could be dynamic during ATP hydrolysis (32). The motions of the THF may contribute to polypeptide translocation in other states.

β-Strand Conformation of the Polypeptide Substrates during Translocation. Clamping at the entrance of SecA induces the β-conformation of the polypeptide substrates. β-strand formation seems to be a common theme in protein translocation. For example, a polypeptide substrate in AAA ATPase Vps4 has been observed to adopt the β-conformation to allow tight engagement with pore loops during translocation (44). Induced β-augmentation is the structural basis for translocation of β-barrel membrane proteins by the bacterial β-barrel assembly machinery (BAM) (57) and by the mitochondrial sorting and assembly machinery (SAM) complex (58). Inhibition of β-sheet formation by a β-peptide mimic during protein translocation through BAM has been proven to be an effective approach in antibiotics development for gram-negative bacteria (59). Considering the critical role of β formation and clamping during SecA-mediated translocation, clogging the clamp by β-peptide mimics could also inhibit protein translocation, suggesting that it could represent a strategy in antibiotic development for both gram-positive and gram-negative bacteria.

Materials and Methods

Detailed materials and methods are reported in *SI Appendix*, Materials and Methods.

Cryo-EM Structure Determination. The assembly, purification, and structure determination of the translocation intermediates followed the method published previously (17) with modifications. In brief, the proOmpA substrate, SecY, and SecA were coexpressed in *Escherichia coli*. The purification of the translocation complex was carried out without delay. ADP and ADP·BeF_3^- were added to the purified complex right before vitrification. All datasets were collected on a 300-kV transmission electron microscope (Titan Krios). "Seed-facilitated 3D classification" was applied during the calculation to improve the resolution (60).

In Vitro Translocation Assay and ATPase Assay. The translocation assays were carried out with the SecY proteoliposomes, SecA mutants, and a polypeptide substrate with the signal sequence from a ribose-binding protein. The ATPase assays of the SecA mutants followed the instruction of the BIOMOL® Green (Enzo) kit.

MD Simulations. The coarsed-grained (CG) MD simulations and all-atom MD simulations were performed sequentially based on the cryo-EM structures of the translocation intermediates, with lipid and water represented explicitly, using the MARTINI 2.2 (61) and the CHARMM36m force fields (62), respectively. Further details are provided in *SI Appendix*, Text.

Data, Materials, and Software Availability. The atomic coordinates and cryo-EM reconstructions have been deposited in the Protein Data Bank under PDB ID 7WHA (with ADP·BeF_3^-) and 7XHB (with ADP), and EMDataBank under ID EMD-33192 (with ADP·BeF_3^-) and EMD-33193 (with ADP). Essential study data are included in the article and/or *SI Appendix*. Additional data and materials are available from the corresponding authors upon reasonable request.

ACKNOWLEDGMENTS. We thank Dr. Tom A. Rapoport for discussion of the project and critical reading of the manuscript, Dr. Ning Gao and Dr. Ningning Li for helping with cryo-EM calculation, Dan Kong and Dr. Chuangye Yan for helping with seed-facilitated 3D classification, and the National Center for Protein Sciences at the Peking University for assistance with protein purification. The cryo-EM data were collected at the cryo-EM platform of the Peking University. The computation was supported by the High-Performance Computing Platform of the Peking University. Part of the MD simulations was performed on the Computing Platform of the Center for Life Sciences at the Peking University. This work was supported by the National Natural Science Foundation of China (NSFC) (31870835 to L.L. and 21873006 to C.S.).

Author affiliations: [a]State Key Laboratory of Membrane Biology, Peking-Tsinghua Center for Life Sciences, School of Life Sciences, Peking University, Beijing 100871, China; and [b]Center for Quantitative Biology, Peking-Tsinghua Center for Life Sciences, Academy for Advanced Interdisciplinary Studies, Peking University, Beijing 100871, China

1. W. Wickner, R. Schekman, Protein translocation across biological membranes. *Science* **310**, 1452–1456 (2005).
2. A. J. Driessen, N. Nouwen, Protein translocation across the bacterial cytoplasmic membrane. *Annu. Rev. Biochem.* **77**, 643–667 (2008).
3. A. Tsirigotaki, J. De Geyter, N. Sostaric, A. Economou, S. Karamanou, Protein export through the bacterial Sec pathway. *Nat. Rev. Microbiol.* **15**, 21–36 (2017).
4. T. A. Rapoport, Protein translocation across the eukaryotic endoplasmic reticulum and bacterial plasma membranes. *Nature* **450**, 663–669 (2007).

5. S. Lang *et al.*, An update on Sec61 channel functions, mechanisms, and related diseases. *Front. Physiol.* **8**, 887 (2017).
6. B. Van den Berg *et al.*, X-ray structure of a protein-conducting channel. *Nature* **427**, 36–44 (2004).
7. R. M. Voorhees, R. S. Hegde, Toward a structural understanding of co-translational protein translocation. *Curr. Opin. Cell Biol.* **41**, 91–99 (2016).
8. R. M. Voorhees, I. S. Fernandez, S. H. Scheres, R. S. Hegde, Structure of the mammalian ribosome-Sec61 complex to 3.4 A resolution. *Cell* **157**, 1632–1643 (2014).
9. M. Gogala *et al.*, Structures of the Sec61 complex engaged in nascent peptide translocation or membrane insertion. *Nature* **506**, 107–110 (2014).
10. L. Bischoff, S. Wickles, O. Berninghausen, E. O. van der Sluis, R. Beckmann, Visualization of a polytopic membrane protein during SecY-mediated membrane insertion. *Nat. Commun.* **5**, 4103 (2014).
11. W. Wickner, A. J. Driessen, F. U. Hartl, The enzymology of protein translocation across the Escherichia coli plasma membrane. *Annu. Rev. Biochem.* **60**, 101–124 (1991).
12. J. Q. Ye, A. R. Osborne, M. Groll, T. A. Rapoport, RecA-like motor ATPases–Lessons from structures. *Biochim. Biophys. Acta* **1659**, 1–18 (2004).
13. J. F. Hunt *et al.*, Nucleotide control of interdomain interactions in the conformational reaction cycle of SecA. *Science* **297**, 2018–2026 (2002).
14. B. W. Bauer, T. A. Rapoport, Mapping polypeptide interactions of the SecA ATPase during translocation. *Proc. Natl. Acad. Sci. U.S.A.* **106**, 20800–20805 (2009).
15. J. Zimmer, Y. Nam, T. A. Rapoport, Structure of a complex of the ATPase SecA and the protein-translocation channel. *Nature* **455**, 936–943 (2008).
16. L. Li *et al.*, Crystal structure of a substrate-engaged SecY protein-translocation channel. *Nature* **531**, 395–399 (2016).
17. C. Ma *et al.*, Structure of the substrate-engaged SecA-SecY protein translocation machine. *Nat. Commun.* **10**, 2872 (2019).
18. M. R. Singleton, M. S. Dillingham, D. B. Wigley, Structure and mechanism of helicases and nucleic acid translocases. *Annu. Rev. Biochem.* **76**, 23–50 (2007).
19. S. S. Velankar, P. Soultanas, M. S. Dillingham, H. S. Subramanya, D. B. Wigley, Crystal structures of complexes of PcrA DNA helicase with a DNA substrate indicate an inchworm mechanism. *Cell* **97**, 75–84 (1999).
20. J. Y. Lee, W. Yang, UvrD helicase unwinds DNA one base pair at a time by a two-part power stroke. *Cell* **127**, 1349–1360 (2006).
21. K. Saikrishnan, B. Powell, N. J. Cook, M. R. Webb, D. B. Wigley, Mechanistic basis of 5′-3′ translocation in SF1B helicases. *Cell* **137**, 849–859 (2009).
22. Y. Gao, W. Yang, Different mechanisms for translocation by monomeric and hexameric helicases. *Curr. Opin. Struct. Biol.* **61**, 25–32 (2020).
23. R. D. Vale, AAA proteins. Lords of the ring. *J. Cell Biol.* **150**, F13–F19 (2000).
24. B. DeLaBarre, J. C. Christianson, R. R. Kopito, A. T. Brunger, Central pore residues mediate the p97/VCP activity required for ERAD. *Mol. Cell* **22**, 451–462 (2006).
25. J. Hinnerwisch, W. A. Fenton, K. J. Furtak, G. W. Farr, A. L. Horwich, Loops in the central channel of ClpA chaperone mediate protein binding, unfolding, and translocation. *Cell* **121**, 1029–1041 (2005).
26. A. Martin, T. A. Baker, R. T. Sauer, Diverse pore loops of the AAA+ ClpX machine mediate unassisted and adaptor-dependent recognition of ssrA-tagged substrates. *Mol. Cell* **29**, 441–450 (2008).
27. C. Puchades *et al.*, Structure of the mitochondrial inner membrane AAA+ protease YME1 gives insight into substrate processing. *Science* **358**, eaao0464 (2017).
28. C. Puchades, C. R. Sandate, G. C. Lander, The molecular principles governing the activity and functional diversity of AAA+ proteins. *Nat. Rev. Mol. Cell Biol.* **21**, 43–58 (2020).
29. W. J. Allen *et al.*, Two-way communication between SecY and SecA suggests a Brownian ratchet mechanism for protein translocation. *Elife* **5**, e15598 (2016).
30. R. A. Corey *et al.*, ATP-induced asymmetric pre-protein folding as a driver of protein translocation through the Sec machinery. *Elife* **8**, e41803 (2019).
31. B. W. Bauer, T. Shemesh, Y. Chen, T. A. Rapoport, A "push and slide" mechanism allows sequence-insensitive translocation of secretory proteins by the SecA ATPase. *Cell* **157**, 1416–1429 (2014).
32. M. A. Catipovic, B. W. Bauer, J. J. Loparo, T. A. Rapoport, Protein translocation by the SecA ATPase occurs by a power-stroke mechanism. *EMBO J.* **38**, e101140 (2019).
33. M. A. Catipovic, T. A. Rapoport, Protease protection assays show polypeptide movement into the SecY channel by power strokes of the SecA ATPase. *EMBO Rep.* **21**, e50905 (2020).
34. A. R. Osborne, W. M. Clemons Jr., T. A. Rapoport, A large conformational change of the translocation ATPase SecA. *Proc. Natl. Acad. Sci. U.S.A.* **101**, 10937–10942 (2004).
35. Y. Papanikolau *et al.*, Structure of dimeric SecA, the Escherichia coli preprotein translocase motor. *J. Mol. Biol.* **366**, 1545–1557 (2007).
36. J. de Keyzer, C. van der Does, T. G. Kloosterman, A. J. M. Driessen, Direct demonstration of ATP-dependent release of SecA from a translocating preprotein by surface plasmon resonance. *J. Biol. Chem.* **278**, 29581–29586 (2003).
37. Z. C. Wu, J. de Keyzer, A. Kedrov, A. J. Driessen, Competitive binding of the SecA ATPase and ribosomes to the SecYEG translocon. *J. Biol. Chem.* **287**, 7885–7895 (2012).
38. S. Koch *et al.*, Lipids activate SecA for high affinity binding to the SecYEG complex. *J. Biol. Chem.* **291**, 22534–22543 (2016).
39. J. D. Pedelacq, S. Cabantous, T. Tran, T. C. Terwilliger, G. S. Waldo, Engineering and characterization of a superfolder green fluorescent protein. *Nat. Biotechnol.* **24**, 79–88 (2006).
40. C. Mitchell, D. Oliver, Two distinct ATP-binding domains are needed to promote protein export by Escherichia coli SecA ATPase. *Mol. Microbiol.* **10**, 483–497 (1993).
41. H. Mori, K. Ito, The long alpha-helix of SecA is important for the ATPase coupling of translocation. *J. Biol. Chem.* **281**, 36249–36256 (2006).
42. K. J. Erlandson *et al.*, A role for the two-helix finger of the SecA ATPase in protein translocation. *Nature* **455**, 984–987 (2008).
43. L. L. Randall, S. J. S. Hardy, Correlation of competence for export with lack of tertiary structure of the mature species - a study invivo of maltose-binding protein in Escherichia-coli. *Cell* **46**, 921–928 (1986).
44. H. Han, N. Monroe, W. I. Sundquist, P. S. Shen, C. P. Hill, The AAA ATPase Vps4 binds ESCRT-III substrates through a repeating array of dipeptide-binding pockets. *Elife* **6**, e31324 (2017).
45. M. Pan *et al.*, Mechanistic insight into substrate processing and allosteric inhibition of human p97. *Nat. Struct. Mol. Biol.* **28**, 614–625 (2021).
46. J. Zimmer, W. Li, T. A. Rapoport, A novel dimer interface and conformational changes revealed by an X-ray structure of Bacillus subtilis SecA. *J. Mol. Biol.* **364**, 259–265 (2006).
47. N. Chada *et al.*, Single-molecule observation of nucleotide induced conformational changes in basal SecA-ATP hydrolysis. *Sci. Adv.* **4**, eaat8797 (2018).
48. Y. Chen, B. W. Bauer, T. A. Rapoport, J. C. Gumbart, Conformational changes of the clamp of the protein translocation ATPase SecA. *J. Mol. Biol.* **427**, 2348–2359 (2015).
49. W. Yang, Lessons learned from UvrD helicase: Mechanism for directional movement. *Annu. Rev. Biophys.* **39**, 367–385 (2010).
50. J. Yu, T. Ha, K. Schulten, How directional translocation is regulated in a DNA helicase motor. *Biophys. J.* **93**, 3783–3797 (2007).
51. E. Schiebel, A. J. M. Driessen, F. U. Hartl, W. Wickner, Delta-mu-H+ and Atp function at different steps of the catalytic cycle of preprotein translocase. *Cell* **64**, 927–939 (1991).
52. K. Sato, H. Mori, M. Yoshida, M. Tagaya, S. Mizushima, Short hydrophobic segments in the mature domain of ProOmpA determine its stepwise movement during translocation across the cytoplasmic membrane of Escherichia coli. *J. Biol. Chem.* **272**, 5880–5886 (1997).
53. K. J. Erlandson, E. Or, A. R. Osborne, T. A. Rapoport, Analysis of polypeptide movement in the SecY channel during SecA-mediated protein translocation. *J. Biol. Chem.* **283**, 15709–15715 (2008).
54. W. J. Allen, D. W. Watkins, M. S. Dillingham, I. Collinson, Refined measurement of SecA-driven protein secretion reveals that translocation is indirectly coupled to ATP turnover. *Proc. Natl. Acad. Sci. U.S.A.* **117**, 31808–31816 (2020).
55. A. Gonsberg *et al.*, The Sec61/SecY complex is inherently deficient in translocating intrinsically disordered proteins. *J. Biol. Chem.* **292**, 21383–21396 (2017).
56. S. Whitehouse *et al.*, Mobility of the SecA 2-helix-finger is not essential for polypeptide translocation via the SecYEG complex. *J. Cell Biol.* **199**, 919–929 (2012).
57. D. Tomasek *et al.*, Structure of a nascent membrane protein as it folds on the BAM complex. *Nature* **583**, 473–478 (2020).
58. Q. Wang *et al.*, Structural insight into the SAM-mediated assembly of the mitochondrial TOM core complex. *Science* **373**, 1377–1381 (2021).
59. H. Kaur *et al.*, The antibiotic darobactin mimics a beta-strand to inhibit outer membrane insertase. *Nature* **593**, 125–129 (2021).
60. N. Wang, Structural basis of human monocarboxylate transporter 1 inhibition by anti-cancer drug candidates. *Cell* **184**, 370–383.e13 (2021), 10.1016/j.cell.2020.11.043.
61. S. J. Marrink, H. J. Risselada, S. Yefimov, D. P. Tieleman, A. H. de Vries, The MARTINI force field: Coarse grained model for biomolecular simulations. *J. Phys. Chem. B* **111**, 7812–7824 (2007).
62. J. Huang *et al.*, CHARMM36m: An improved force field for folded and intrinsically disordered proteins. *Nat. Methods* **14**, 71–73 (2017).